Chapter 4

Photoinduced Oligomerization of Aqueous Pyruvic Acid

Abstract

The 320 nm band photodecarboxylation of aqueous pyruvic acid, PA, a representative of the α-oxocarboxylic acids widely found in the atmospheric aerosol, yields 2,3-dimethyl tartaric, *A*, and 2-(3-oxobutan-2-yloxy)-2-hydroxypropanoic, *B*, acids, rather than 3-hydroxy-2-oxobutanone as previously reported. *A* and *B* are identified by liquid chromatography with UV and ESI MS detection, complemented by collisional induced dissociation and ^{2}H- and ^{13}C-isotope labeling experiments. The multifunctional ether *B* gives rise to characteristic δ ~ 80 ppm ^{13}C-NMR resonances. Quantum yields of product formation increase with PA concentration as $[PA](a + [PA])^{-1}$ in the range $5 \leq [PA]/mM \leq 100$. CO_2(g) release rates are halved, while *A* and *B* are suppressed by the addition of > 1.5 mM TEMPO. *A* and *B* are only partially quenched in air-saturated solutions. These observations are shown to be consistent with an oligomerization process initiated by a bimolecular reaction between ^{3}PA* and PA producing ketyl, $CH_3\dot{C}(OH)C(O)OH$, and acetyl, $CH_3C(O)\cdot$, radicals, rather than by the unimolecular decomposition of $^{3}PA^{*}$ into 1-hydroxyethylidene, $^{3}HO(CH_3)C$: (+ CO_2), or $[CH_3C(O)\cdot + \cdot C(O)OH]$ pairs. *A* arises from the dimerization of ketyl radicals, while *B* ensues from the facile decarboxylation of the C_8β-ketoacid formed by association of acetyl radicals with the ketyl radical adduct of PA. Since the radical precursors to *A* and *B* are scavenged by O_2 with a low probability per encounter ($k_{sc} \sim 1 \times 10^{6}\ M^{-1}\ s^{-1}$), PA is able to accrete into multifunctional polar species in aerated aqueous media under solar illumination.

Keywords: Pyruvic acid, photolysis, α-oxocarboxylic, oligomerization.

Introduction

Pyruvic acid, PA, and other α-dicarbonyls are ubiquitous components of surface waters and the atmospheric aerosol.[1-7] They are globally produced in the photochemical degradation of the colored organic matter tinting rivers, lakes, and oceans,[8] and in the atmospheric oxidation of organic gases and vapors.[9] Their fate is, however, uncertain. Species containing α-dicarbonyl moieties absorb light above $\lambda \sim 300$ nm, i.e.,[10] they are potentially sensitive to sunlight.[11,12] In water, however, most α-dicarbonyls, with the exception of PA that substantially (~ 35% at 298 K) retains its ketonic functionality, are largely hydrated into transparent *gem*-diols.[13,14] Excitation of the $n \rightarrow \pi^*$ band of aqueous PA ($\varepsilon_{max} = 11.3\ M^{-1}\ cm^{-1}$ at 321 nm) induces its efficient photodecarboxylation:[15]

$$CH_3C(O)C(O)OH + h\nu \rightarrow\rightarrow {}^3[CH_3C(O)C(O)OH]^* \rightarrow\rightarrow CO_2 + \text{other products} \quad (4\text{-}1)$$

The identity of the "other products" and the mechanism of this seemingly simple process remain, however, controversial.[16,17] Early studies reported that 3-hydroxy-2-oxobutanone (acetoin) is the main organic product, that pyruvate [pK_a(PA) = 2.4] is considerably more photostable than PA,[15] and proposed that reaction 4-1 proceeds via the concerted decarboxylation of ^{3}PA* into triplet 1-hydroxyethylidene, $^3HO(CH_3)C$:. While a concerted process likely accounts for the exclusive formation of acetaldehyde in the photolysis (and thermolysis) of PA in the gas phase,[15,18-21] and in the related photodecarboxylation of aqueous benzoylformic acid into benzaldehyde,[22] it is not apparent why $^3HO(CH_3)C$: would fail to rapidly rearrange into acetaldehyde in water as it does in the gas phase.[21] Closs and Miller, C&M,[23] interpreted that their CIDNP

experiments were consistent with ^{3}PA* α-cleavage into ^{3}[$CH_3C(O)\cdot$ $\cdot COOH$] geminate radical pairs, followed by the release of CO_2 during the subsequent reduction of PA by ·COOH. The association of the resulting ketyl and acetyl radicals would lead to 2-methyl-2-hydroxy-3-oxobutanoic acid (2-acetolactic, 2-AL), a marginally stable β-ketoacid that decarboxylates into acetoin within minutes at ambient temperature.[23,24]

A remarkable aspect of PA photochemistry is its sensitivity to the medium. Thus, PA is photostable in deareated benzene, but is photoxidized to peracetic acid in the presence of O_2.[25] In methanol and other hydrogen-donating solvents (even in *t*-butanol) PA behaves as a typical ketone, being photoreduced to 2,3-dimethyltartaric and 2-methyl-2,3-dihydroxypropanoic acids without significant decarboxylation.[26] The noticeable enhancement of PA decarboxylation rates in benzene upon doping with pyridine led Davidson et al. to suggest, and explore via kinetic spectroscopy, the possibility that in inert polar solvents, such as water, the reaction actually proceeds via intermolecular photoinduced electron transfer (PET) between ^{3}PA* and PA.[27-29] Since electron transfer from ^{3}PA* (E_T = 3.0 eV)[30] to PA leading to $PA^{+\cdot}$ (E^0 ~ 3.5 V)[31] plus $PA^{-\cdot}$ is thermochemically disallowed, the process likely involves proton-coupled electron transfer,[32,33] which is equivalent to H-atom transfer. A similar mechanism may apply to other carbonyls in water.[34] A bimolecular process should be favored at high PA concentrations, such as those prevailing in the atmospheric aerosol, over the unimolecular type-1 homolysis taking place in surface waters and, possibly, in cloud droplets.[35,36] The transition from a unimolecular to a bimolecular initiation mechanism is expected to occur above ~ 10 mM PA, when the (reactive) quenching of ^{3}PA* by PA ($k_Q = 2 \times 10^8$ M^{-1} s^{-1}) becomes competitive with ^{3}PA* spontaneous decay ($k_{decay} = 2 \times 10^6$ M^{-1} s^{-1}).[28]

We recently reported that frozen aqueous PA glasses UV-irradiated at 77 K exhibit paramagnetic signals corresponding to distant (i.e., separated by > 0.5 nm) triplet radical pairs that persist up to ~ 190 K[37] The formation of distant triplet-correlated radicals in low-temperature glasses, where PA is largely associated into hydrogen-bonded cyclic dimers, is only possible via long-range (proton-coupled) electron transfer between carbonyl groups, i.e., via a bimolecular charge transfer process related to that proposed by Davidson et al.[27-29] Here, we report that the stable products formed in the 320 nm band photolysis of acidic, aqueous $5 \leq [PA]/mM \leq 100$ solutions at 293 K are thermolabile C_6 and C_7 oligomers whose identification requires the use of soft analytical techniques, and we propose a reaction mechanism accounting for all observations.

Experimental Section

0.1 M PA (Aldrich 98.0%, bidistilled at reduced pressure) or 10.0 mM benzoylformic acid (Aldrich 97%, used as received), BF, solutions in Milli-Q water (18.2 MΩ cm^{-1}) were acidified to pH 1.0 with perchloric acid (Mallinckrodt, 70% analytical reagent) prior to photolysis. About 35 % PA is in its photoactive keto-form in water at 293 K.[13,14] These solutions were photolyzed in a sealed reactor to monitor the release of CO_2(g) via online absorption infrared spectrophotometry at 2349 cm^{-1}. This photochemical reactor, a cylindrical chamber provided with an axial silica finger housing the lamp (Hg Pen-Ray model CPQ 8064, emitting at 313 ± 20 nm) was coupled to an infrared cell (CaF_2 windows, 10 cm path; Bio-Rad Digilab FTS-45 FTIR spectrometer) via a circulating micropump (Schwartzer miniature pump model 135 FZ) for the continuous analysis of

gas-phase products. The gas filling the entire (reactor + cell) volume was recirculated every ~ 4 s. PA or BF solutions (4 mL) were sparged in the reactor with ultrapure N_2 for 30 min prior to photolysis, and then sealed. Solutions were magnetically stirred during photolysis. More than 98% of the CO_2 formed in reaction 4-1 is released into the gas-phase at pH 1.0, while organic products remain in solution. Photolysis experiments were alternatively carried out on solutions contained in 3.5 mL silica UV cuvettes under continuous gas sparging, which were irradiated with light from a 1 kW high-pressure Xe-Hg lamp filtered through a $\lambda = 320 \pm 10$ nm band-pass interference filter (Oriel) and a water filter to remove unwanted infrared radiation. All experiments were performed at 293 K.

We also studied the thermal decarboxylation of aqueous 2-AL in the photochemical reactor at 293 K. 2-AL was prepared by hydrolysis of its methyl ester (Aldrich 98%) in 0.1 M NaOH at 274 K.[24,38] A portion of this sodium 2-acetolactate solution was diluted to 2.5 mM with ultrapure water at 274 K, and transferred to the photochemical reactor. After sealing the reactor, the solution was acidified to pH 1.0 with perchloric acid injected through a septum port and rapidly thermalized at 293 K. Aqueous solutions of the radical scavenger 2,2,6,6-tetramethylpiperidin-1-oxyl (TEMPO, Aldrich 99%, purified by vacuum sublimation) were used in some experiments. At concentrations below 4 mM, TEMPO intercepts less than 5% of the light absorbed by 0.1 M PA at $\lambda \sim$ 320 nm.

Organic product analyses were performed by means of liquid chromatography at ambient temperature, using UV and electrospray ionization-mass spectrometric detection (ESI MS) (Agilent 1100 series Model 1100 Series HPLC-MSD System). A ZORVAX

Eclipse XDB-C18 column (3 × 250, 5 μm, Agilent), operated under isocratic conditions (0.4 mL min^{-1}; 0.925 CHCOOH 0.1% + 0.075 CH_3OH; 0 to 8 min) followed by gradient elution (up to 0.075 CHCOOH 0.1% + 0.925 CH_3OH; 8 to 21 min) was used in these separations. The electrospray ionization inlet was set to detect negative ions in the range of 65 to 1000 Da.

Gas chromatography–mass spectrometric analysis (Hewlett-Packard 6890 GC-5973 MSD system) were carried out using a polar polyethylene glycol (PEG) HP-INNOWax capillary column (30 m long, 0.25 mm i.d., coated with a 0.25 μm stationary phase film; injector at 250 °C; column temperature: 65 °C for 2 min, heating at 5 °C/min up to 100 °C, then at 25 °C/min up to 220 °C) with 70 eV electron impact ionization. Samples for analysis were prepared by mixing the analyte (250 μL) with 0.2 mM hexanol in acetonitrile as internal standard (500 μL), and acetonitrile (250 μL).

Organic product mixtures were also analyzed by ^{13}C NMR (75 MHz Varian 300 spectrometer). $^{13}C_3$-PA (Cambridge Isotope Laboratories, 99% $^{13}C_3$) solutions (in ultrapure water + 20% D_2O, pH 1.0) contained in sealable tubes (RotoTite, Wilmad) were degassed via freeze-and-thaw cycles under vacuum, and then irradiated for 2 h at 293 K with the (1 kW Xe-Hg lamp plus λ = 320 nm filter) source described above.

Results and Discussion

Rates of CO_2 Formation

The evolution of CO_2(g) from deareated aqueous 0.1 M PA at pH 1.0 under continuous illumination is shown in Fig. 4-1. Neither CO nor CH_4, which would absorb at 2169 cm^{-1} and 3019 cm^{-1}, respectively, were formed in these experiments.[39] The CO_2

concentration values plotted in Fig. 4-1 correspond to moles of CO_2 produced divided by the volume of the aqueous PA solution (4 mL), which were obtained from integrated 2349 cm^{-1} absorption band intensities. Similar measurements for the rate of CO_2(g) released in the photolysis of deareated BF, reaction 4-2:

$$C_6H_5C(O)C(O)OH + h\nu \rightarrow CO_2 + C_6H_5C(H)O \qquad (4\text{-}2)$$

together with the evaluation of the effective absorption coefficients, ε_{eff}'s, of PA and BF from the convolution of their experimental absorption spectra with the emission spectrum of the lamp, –instead of measuring BF decay rates by absorption spectrophotometry at λ = 350 nm–,[40] and the recently reevaluated quantum yield of reaction (4-2): $\phi_{4\text{-}2}$ = 0.38,[22] lead to $\phi_{4\text{-}1}$ = 0.78 ± 0.10, in excellent agreement with the $\phi_{4\text{-}1}$ = 0.79 value previously reported.[15]

To test the validity of C&M's mechanism of CO_2 production in reaction 4-1 and reactions 4-3–4-5:

$$^3[CH_3C(O)C(O)OH]^* \rightarrow {}^3[CH_3C(O)\bullet \ \bullet C(O)OH]_{cage} \rightarrow CH_3C(O)\bullet + \bullet C(O)OH \qquad (4\text{-}3)$$

$$CH_3C(O)C(O)OH + \bullet C(O)OH \rightarrow CO_2 + CH_3\dot{C}(OH)C(O)OH \qquad (4\text{-}4)$$

$$CH_3\dot{C}(OH)C(O)OH + CH_3C(O)\bullet \rightarrow \text{2-AL} \rightarrow CH_3C(OH)C(O)CH_3 + CO_2 \qquad (4\text{-}5)$$

we investigated the effect of the radical scavenger TEMPO on the initial rates of CO_2(g) evolution, R_{CO_2}, from irradiated 0.1 M PA solutions under 1 atm N_2 at 293 K (Figs. 4-1 and 4-2). R_{CO_2} was found to decrease linearly with increasing TEMPO initial

concentration before bottoming out at $R_{CO_2,\infty} \sim 0.45\ R_{CO_2,0}$ for $[TEMPO]_{lim} \sim 1.7$ mM (Fig. 4-2). The endothermic decomposition of thermalized ·C(O)OH radicals:

$$\cdot C(O)OH \rightarrow CO_2 + \cdot H \qquad (4\text{-}6)$$

with $\Delta H_{4\text{-}6} \sim 46$ kJ mol^{-1}, $E_{4\text{-}6} \sim 146$ kJ mol^{-1}, $A_{4\text{-}6} \sim 10^{13}$ s^{-1},[39] is exceedingly slow in condensed phases at 293 K. Therefore, ·C(O)OH could only generate CO_2 by either reducing PA, reaction 4-4, or TEMPO, reaction 4-7:

$$TEMPO\cdot + \cdot C(O)OH \rightarrow CO_2 + TEMPO\text{-}H \qquad (4\text{-}7)$$

where TEMPO· depicts TEMPO as an O-centered free radical, and TEMPO-H represents the hydroxylamine resulting from H-abstraction by the nitroxyl group. If reaction 4-4 were so fast that ~ 2 mM TEMPO could not compete with 0.1 M PA toward ·C(O)OH, then TEMPO should have no effect on R_{CO_2} because, by failing to scavenge ·C(O)OH, it could not arrest the formation of the additional CO_2 produced in reaction 4-5. Therefore, within this scheme, the fact that TEMPO has a detrimental effect on R_{CO_2} requires that reactions 4-4 and 4-7 have competitive rates under the present conditions (although we estimate, from $k_{4\text{-}7} \sim 3 \times 10^9$ M^{-1} s^{-1},[35] $k_{4\text{-}4} < 1 \times 10^4$ M^{-1} s^{-1},[41] that $k_{4\text{-}7}\,[TEMPO]_{lim} \sim 6 \times 10^6$ s^{-1} >> $k_{4\text{-}4}\,[PA] < 1 \times 10^3$ s^{-1}). Thus, by effectively scavenging ·C(O)OH via reaction 4-7 and, hence, by preventing the occurrence of reaction 4-5, TEMPO could indeed limit R_{CO_2} to about half the rates measured in the unscavenged system. However, if that were the case, since TEMPO also acts as a physical quencher of ^{3}PA* in this concentration range, as observed during the photolysis of 0.33 mM PA at [TEMPO] > 0.5 mM,[35] $R_{CO_2,\infty}$ should tend to 0 rather than to 0.45 $R_{CO_2,0}$! Therefore, the fact that TEMPO fails to fully

quench R_{CO_2} rules out reaction 4-4 as the source of CO_2 under present conditions. The results of Fig. 4-2 seem to require instead that about half of the CO_2 produced in reaction 4-1 be formed at rates much faster than the frequency of reactive encounters with < 4 mM TEMPO, and the remainder via free radicals that are fully scavenged by ~ 2 mM TEMPO. PA solutions previously sparged with 1 atm O_2 release CO_2 at rates ~ 25% smaller than from deareated solutions.

Further verification of the shortcomings of C&M's proposal, reactions 4-3–4-5, is provided by the slow decarboxylation of 2-AL vs. the lack of post-illumination CO_2(g) in PA photolysis (Fig. 4-3). If 2-AL acid were the intermediate responsible for the quenchable portion of CO_2 production in the photolysis of PA (Figs. 4-1 and 4-2), we should have detected the release of significant amounts of CO_2 after illumination, at variance with observations. We conclude that the CIDNP signal polarizations induced during PA photolysis in water may be consistent with the association of free radicals arising from ^{3}PA* α-cleavage, reaction 4-3,[23] but do not exclude other reaction pathways or provide any information about their relative contributions under specific conditions.

Organic Product Identification

A liquid chromatogram of photolyzed PA solutions is shown in Figure 4-4. The displayed chromatogram was obtained via ESI with negative ion mass spectral detection. A similar chromatogram is obtained by using UV detection at λ = 254 nm. The only products formed in these experiments elute at 4.1 min (*A*) and 6.9 min (*B*), which are characterized by their UV absorption (Fig. 4-5) and mass (Figs. 4-6) spectra. We checked that acetoin elutes at 5.3 min and, therefore, could have been detected by UV absorption (λ_{max} = 276 nm) if formed. LC of PA photolyzates using positive ion mass spectral

detection did not reveal products other than those shown in Fig. 4-4. The mass spectra of *A* and *B* obtained in the photolysis of $^{13}C_3$-PA solutions in H_2O:D_2O 0.8:0.2 are shown in Figs. 4-6D and 4-6F, respectively.

It is apparent that *A* corresponds to a C_6-carboxylic acid of molecular mass 178 Da, because *A* is detected by negative ion mass spectrometry as its conjugated base $(A - H)^-$ at $m/z^- = 177$, or at 183 Da (Figs. 4-6C and 6D) depending on whether it is produced in the photolysis of $^{12}C_3$-PA or $^{13}C_3$-PA, respectively. *A* lacks chromophores absorbing above $\lambda \sim 250$ nm (Fig. 4-5C) and, furthermore, carries ~ six deuterons that are not readily exchangeable with the eluent during HPLC analysis (Fig. 4-6D). This conclusion is based on the fact that PA exchanges all its protons, including the methyl protons, with partially deuterated water at pH 1.0 via acid-catalyzed enolization.[42] However, the labeling of its methyl protons is largely preserved during analysis using a weakly acidic eluent. Hence, the $\rho = I_{M+1}/I_M = I_{91}/I_{90} = 0.182$ ratio in the mass spectrum of $^{13}C_3$-PA solutions prepared in partially deuterated water (Fig. 4-6B) gauges the extent of deuteration of its methyl group. The fact that $\rho = I_{M+1}/I_M = I_{184}/I_{183} = 0.347 \sim (2 \times 0.182)$, in the mass spectrum of $^{13}C_6$-*A* (Fig. 4-6D) supports the presence of two methyl groups.

The collision-induced dissociation, CID, of $(A - H)^-$ accelerated at 100 V leads to three prominent negatively charged fragments of $m/z^- = 131$, 115, and 87 Da (Fig. 4-6G). Dicarboxylic acids readily lose CO_2 (m/z = 44) by CID unless they possess α-hydroxyls.[43,44] For example, the CID spectrum of the tartaric acid monoanion, in which both carboxyls are flanked by α-hydroxyls, only undergoes m/z = 46, 62, and 90 losses. The appearance of a 115 $[(A - H)^- - CO_2 - H_2O]$ negative fragment in the CID spectrum of *A* is actually indicative of the presence of two carboxyl groups.[45] We verified that 2,3-

dihydroxy-2,3-dimethyl succinic acid (dimethyl tartaric acid), obtained by photoreduction of PA in methanol solution,[15] also elutes at 4.1 min, and has a 100 V CID spectrum identical to that in Fig. 4-6G.

A similar analysis indicates that *B*: (1) is a C_7-carboxylic acid of mass 176 Da that preserves three intact methyl groups from the PA precursor (Figs. 4-6E and 4-6F) and, (2) possesses, in contrast with *A*, a carbonyl chromophore absorbing at $\lambda_{max} \sim 285$ nm (cf. $\lambda_{max} \sim 276$ nm for acetoin) (Fig. 4-5B). The appearance of a single fragment at $m/z^- = 87$ Da $(PA - H)^-$, i.e., the absence of a $m/z^- = 113$ $[(PA - H)^- - CO_2 - H_2O]$, in the CID mass spectrum of *B* (Fig. 4-6H) suggests the presence of only one carboxyl group.

The 320 nm irradiation of 0.1 M $^{13}C_3$-PA solutions for 2 h led to a mixture whose ^{13}C-NMR spectrum (Fig. 4-7C) reveals the presence of: (1) carboxyl groups at $\delta = 170.4$ and $\delta = 180.1$ ppm (vs. 167.8 ppm in keto-PA and 174.9 in 2,2-dihydroxypropionic acid, DHPA, the *gem*-diol of PA, Fig. 4-7A),[46] (2) carbonyl groups at $\delta = 204.2$ and 217.4 ppm (vs. 215.5 ppm for acetoin and 201.5 for PA, Figs. 4-7B and 4-7A, respectively) that confirm the absence of acetoin and, (3) a group of ether signals in the range $\delta = 78$ to 84 ppm. The latter are in agreement with the resonances found in the products of the anionic polymerization of aqueous PA into linear polyethers.[47-49] The strong signal at 124.8 ppm in Fig. 4-7C corresponds to the CO_2 product.

Effect of Radical Scavengers

The detrimental effect of radical scavengers, such as O_2 and TEMPO, on the formation of *A* and *B* confirms the involvement of free radicals in this system. Both *A* and *B* are still formed in detectable amounts in samples vigorously sparged with air, but they are effectively suppressed under continuous sparging with 1 atm O_2, or by the addition of

2.5 mM TEMPO. From actual photochemical radical initiation rates: $R_i \sim 1.4 \times 10^{-5}$ M s^{-1} (2.5% PA losses after 3 min irradiation of deareated 0.1 M PA), by assuming diffusion-controlled radical recombination rate constants: $k_{rec} \sim 2 \times 10^9$ M^{-1} s^{-1}, we obtain steady-state radical concentrations: $[X\cdot] \sim 6 \times 10^{-8}$ M. The observation that the yields of *A* and *B*, the products of radical recombinations ($X\cdot + X\cdot \rightarrow\rightarrow$ *A* or *B*, see Scheme 4-1), drop fourfold in air ($[O_2]_{aq} = 2.8 \times 10^{-4}$ M),[50] i.e.: $k_{sc}\,[X\cdot]\,[O_2]/(k_{rec}\,[X\cdot]^2) \sim 3$, implies, therefore, that the relevant radicals are effectively scavenged by O_2 with rate constants: $k_{sc}\,(X\cdot + O_2) \sim 1 \times 10^6$ M^{-1} s^{-1}, which are 1000 times smaller than typical diffusion-controlled k_{sc}'s for the scavenging of simple C-centered radicals by O_2.[51-55] From the experiments shown in Fig. 4-1, which involve weaker irradiances, we infer k_{sc}'s for radical scavenging by TEMPO that are somewhat smaller than for O_2. The observed linear R_{CO_2} vs. $[TEMPO]_0$ (Fig. 4-2), rather than a Stern-Volmer $1/R_{CO_2}$ vs. $1/[TEMPO]_0$, dependence, and the fact that the release of CO_2 is inhibited even after $[CO_2] > [TEMPO]_0$ (Fig. 4-1), both suggest that the mechanism of inhibition involves more than a simple ($X\cdot$ + TEMPO) recombination. Since the formation of *A* and *B* ultimately requires alkyl radical recombinations (see below), the possible competition between radical reactions with O_2 vs. addition to PA does not affect the above estimates for k_{sc} in our system. The fact that neither $\sim 3 \times 10^{-4}$ M O_2 nor ca. 2 mM TEMPO are able to quench ^{1,3}PA* states in the presence of 100 mM PA strongly suggests that PA itself acts as a reactive quencher.

Pyruvic Acid Concentration Effects

Previous studies of the dependence of acetyl radical formation rates on PA concentration during the photochemical decomposition of pyruvate solutions were performed in the submicromolar to millimolar range at pH 8.2.[35] The rate of photon absorption by PA solutions, I_a, is given by Equation 4-8:

$$I_a = I_0\ [1 - \exp(-2.303\varepsilon l c)] \qquad (4\text{-}8)$$

where I_0 is the incident photon rate (in M s^{-1}), ε the decadic absorption coefficient, *l* the optical path length, and $c \equiv$ [PA]. For $\varepsilon = \varepsilon_{max} = 11.3\ M^{-1}\ cm^{-1}$, $l = 1$ cm, I_a remains proportional to $[PA]^1$ at [PA] < 4 mM. Under such conditions, therefore, the formation rates of products resulting from species generated in the unimolecular decomposition of ^{3}PA* should increase linearly with [PA], as observed.[35] The corresponding quantum yields, ϕ, should, of course, be independent of [PA].

Typical PA concentrations in atmospheric aerosols exceed, however, the range covered in Ref. 35. For example, Kawamura et al. report $[PA]/[SO_4^{2-}] \sim 1 \times 10^{-3}$ molar ratios in Arctic aerosols,[4] and even larger ratios in urban aerosols.[5] Assuming that the upper limit to the water content of aerosol droplets is determined by the deliquescence curve of ammonium bisulfate solutions,[56] an Arctic aerosol at 50% relative humidity will consist of droplets containing 0.6 g H_2O/g SO_4^{2-}, or > 20 mM PA under very acidic conditions.[57] The normalized sums of the quantum yields of formation of *A* and *B*, $\phi_A + \phi_B$, namely, the sums of their formation rates divided by I_a (from eq. 4-8) normalized to the condition $(\phi_A + \phi_B) \rightarrow 1$ as [PA] $\rightarrow \infty$, measured in irradiated $5 \leq [PA]/mM \leq 100$ solutions at pH 1, are shown in Fig. 4-8. It is apparent that $\phi_A + \phi_B$ is not independent of

[PA] above 5 mM, but increases as [PA](158 + [PA])$^{-1}$. The branching ratio ϕ_B/ϕ_A also increases with [PA], as expected for the competition between the formation rates of a species (*B*) involving radical addition to a third PA vs. the product (*A*) of the recombination of primary radicals. The implication is that the mechanism of photolysis of aqueous PA under present conditions is different than in more dilute solutions and probably involves a bimolecular initiation process.

Mechanism of Reaction

The above results can be rationalized in terms of the mechanism shown in Scheme 4-1 shown on page 4-24. The initiation may involve photoinduced electron transfer between $^3PA^*$ and ground state PA into a bound radical ion pair,[27-29,58] as shown, or proceed via a proton-coupled electron transfer. Either pathway, whose net result is the formation of ketyl, $CH_3\dot{C}(OH)C(O)OH$ (K·), and acyloxyl, $CH_3C(O)C(O)O\cdot$, radicals in a single reactive (^{3}PA* + PA) encounter, could account for present observations. Thermochemical estimates indicate, however, that PA (Δ_fH = 534 kJ mol^{-1}) decompositions into [$CH_3C(O)\cdot$ + ·C(O)OH] or [$^3HO(CH_3)C$:+ CO_2] in the gas phase are 304 kJ mol^{-1} and 326 kJ mol^{-1} endothermic,[39,59] respectively, i.e., that they exceed the excitation energy of ^{3}PA* (E_T = 289 kJ mol^{-1} = 3.0 eV), although they remain accessible to a ^{1}PA* state excited by 320 nm photons (E_S = 372 kJ mol^{-1} = 3.9 eV). These estimates assume that the heats of reactions involving uncharged species should not vary much from the gas phase to aqueous media. On the other hand, as indicated above, the sum of the estimated reduction potentials of the radical ions produced by direct PET between two PA molecules most likely exceeds E_T.[31] A neutral bimolecular channel: 2 PA $\rightarrow$ K· +

$CH_3C(O)C(O)O\cdot$, ΔH = 303 kJ mol^{-1}, is also marginally accessible to triplet excitation, but the concomitant decarboxylation of $CH_3C(O)C(O)O\cdot$ into $CH_3C(O)\cdot + CO_2$ makes the overall process quite favorable. Experiments in solvents of dissimilar polarity,[60] or the direct identification of primary radical ion intermediates may resolve this issue. Regardless of whether the $CH_3C(O)C(O)O\cdot$ radical ensues electron transfer, proton-coupled electron transfer, or H-atom transfer processes, the fact remains that its ultrafast decarboxylation ($k_{4\text{-}9} \sim 10^{12}$ s^{-1}):[61,62]

$$CH_3C(O)C(O)O\bullet \rightarrow CO_2 + CH_3CO\bullet \qquad (4\text{-}9)$$

could not be intercepted by any of the radical scavengers used under present conditions.[63,64] The acetyl radical is rather stable to decarbonylation ($CH_3CO\cdot \rightarrow CH_3\cdot$ + CO, $k_{dec} \sim 0.01$ to 1 s^{-1})[65,66] but is rapidly hydrated in aqueous solution.[67] According to Scheme 4-1, *A* is formed in the self-association of K· radicals.[68-70] The formation of *B* involves the addition of *K*· to PA, either to the keto-form or its enol, followed by the subsequent association of *C* with the acetyl radical into the multifunctional dicarboxylic acid, *D* (220 Da). The rapid decarboxylation of *D* may proceed from the β-oxocarboxyl moiety into *B1*,[71-73] or, less likely, from the α-hydroxycarboxyl moiety into *B2*. The end products of *D* decarboxylation contain: (1) carbonyl groups, which give rise to the $\delta >$ 200 ppm signals in Fig. 4-7C, and to the absorption spectrum of Fig. 4-5B and, (2) ether functionalities, apparent at $\delta \sim 80$ ppm. The decarboxylation of *D* is the source of the CO_2 fraction that can be quenched by radical scavengers. *A* and *B* are thermally labile species that decompose into acetic acid, CO_2, and acetoin during conventional, high-temperature GC-MS analysis.

The results of Fig. 4-8 can be analyzed in terms of a three-step mechanism:

$$PA + h\nu \rightarrow PA^* \quad (4\text{-}10)$$

$$PA^* \rightarrow PA \quad (4\text{-}11)$$

$$PA^* + PA \rightarrow X\cdot + Y\cdot \quad (4\text{-}12)$$

followed by $X\cdot + Y\cdot \rightarrow\rightarrow A + B$, etc, which encapsulates the essence of Scheme 4-1 and the preceding discussion. At steady state, $[PA^*] = I_a \times (k_{4\text{-}11} + k_{4\text{-}12}\,[PA])^{-1}$, and the overall rate of product formation is given by $R_{4\text{-}12} = I_a \times k_{4\text{-}12}\,[PA] \times (k_{4\text{-}11} + k_{4\text{-}12}\,[PA])^{-1}$, or $\phi_{A+B} = R_{4\text{-}12}/\, I_a \propto [PA]\,(a + [PA])^{-1}$, $a = k_{4\text{-}11}/\, k_{4\text{-}12}$, as observed. Reaction 4-11 may involve deactivation, as shown, and/or decomposition into species not convertible into *A* and *B*.

The fact that the products of PA photolysis are inefficiently inhibited by paramagnetic scavengers such as O_2 and TEMPO is a remarkable finding because both the acetyl radical hydrate, $CH_3\dot{C}(OH)_2$, and the ketyl radical anion $K\cdot^-$, $CH_3\dot{C}(OH)C(O)O^-$,[74] are known to rapidly react with O_2: $k_{sc}[CH_3\dot{C}(OH)_2 + O_2] = 7.7 \times 10^8\ M^{-1}\ s^{-1}$,[75] $k_{sc}(K\cdot^- + O_2) = 2.6 \times 10^9\ M^{-1}\ s^{-1}$.[51,74] Some delocalized alkyl radicals, such as the methyl radical derived from N-nitrosodimethylamine: $k_{sc} = 5.3 \times 10^6\ M^{-1}\ s^{-1}$,[76] react with O_2 in water with rate constants that are considerably smaller than the diffusion-controlled limit. The apparently low scavenging efficiencies observed in the present system should probably be ascribed, however, to other effects, such as radical stabilization via inter/intramolecular hydrogen bonding, or the lack of reactive pathways for the peroxyl radicals involved. For example, monofunctional ketyl peroxyl radicals readily split

$HO_2\cdot$.[77] If $KO_2\cdot$ behaved similarly, *A* and *B* formation should have been suppressed in air-saturated solutions, at variance with our results. In this case, however, intramolecular hydrogen bonding is known to hinder internal rotation about the $CH_3\dot{C}(OH)-C(O)OH$ bond in the ESR time scale.[78] Intramolecular hydrogen bonding within the $[\dot{C}(OH)\text{-}C(O)]$ moiety should stabilize K·, possibly retard its association with O_2 (and/or shift the equilibrium: $K + O_2 \rightleftarrows KO_2\bullet$), and hamper $HO_2\cdot$ elimination from $KO_2\cdot$. On the other hand, H-atom abstraction by peroxyl radicals, such as $CH_3C(OH)_2O_2\bullet$, is expected to be endothermic by more than 40 kJ mol^{-1} in the case of PA as substrate.[79]

The apparent sluggishness of O_2 as a radical scavenger may, therefore, be actually associated with the fate of the derived alkylperoxyl radicals. Monofunctional α-hydroxyalkyl radicals react very rapidly with O_2,[80] but the scavenging of free radicals by sorbitol, a C_6 polyol, via H-atom abstraction leads to multifunctional ketyl radicals that undergo competitive crosslinking even in the presence of O_2.[81] The free radical scavenging activity of sugars,[82-84] and related species may be a general phenomenon associated with the inability of polyhydroxylic alkyl radicals to propagate oxidative chains in water. Further work is underway.

Acknowledgment: This work was financed by NSF grant ATM-0228140. This project benefited from the use of instrumentation made available by the Caltech Environmental Analysis Center. N. Dalleska provided valuable assistance with chromatographic analysis.

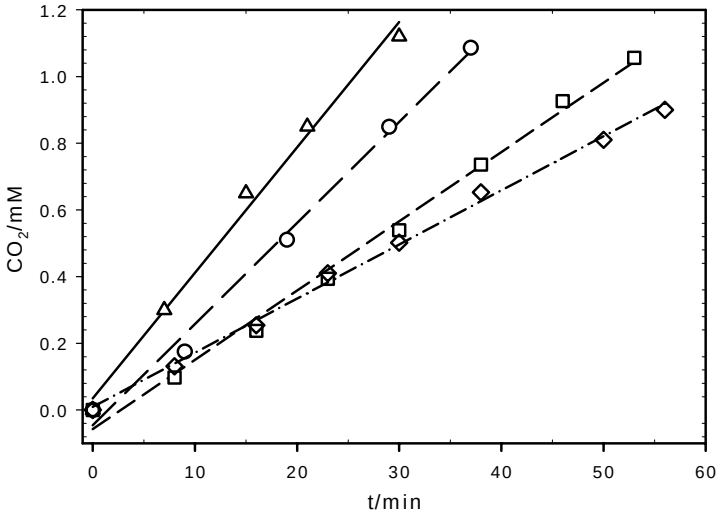

Figure 4-1. CO_2(g) evolution during the 313 nm photolysis of deareated aqueous 0.1 M PA solutions at 293 K in the presence of various TEMPO initial concentrations. $[TEMPO]_0$/mM = 0 (△); 0.50 (○); 1.36 (□); 1.71 (◊).

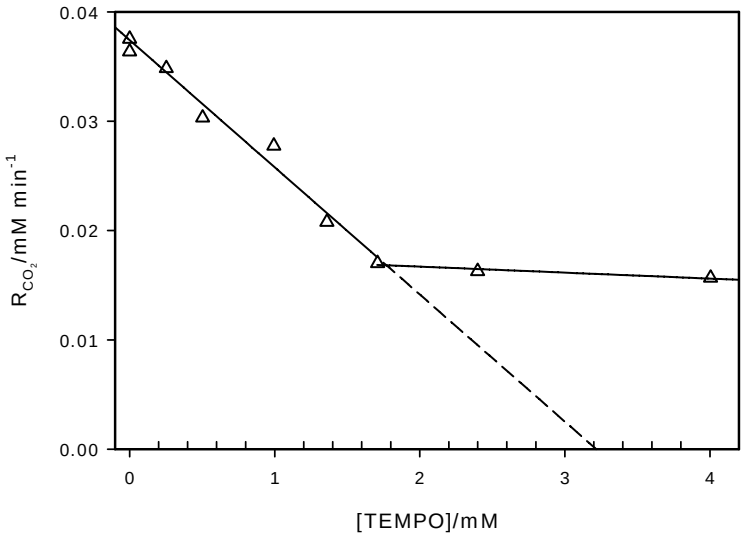

Figure 4-2. Rates of CO_2(g) evolution, R_{CO_2}, vs. $[TEMPO]_0$ for the 313 nm photolysis of deareated 0.1 M PA aqueous solutions at 293 K.

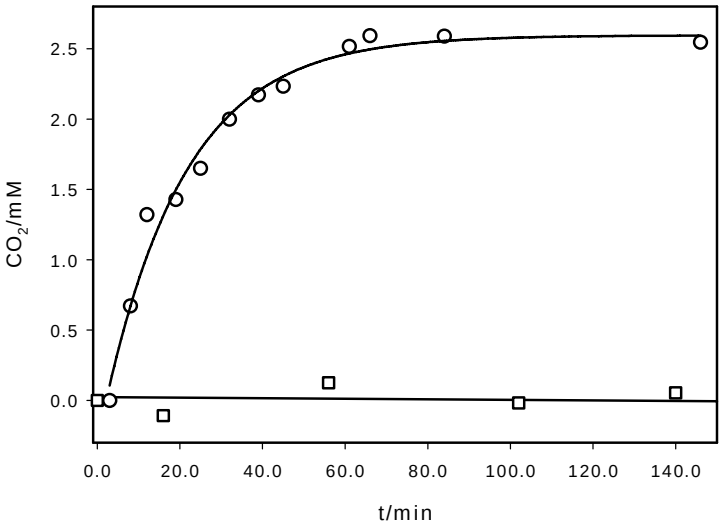

Figure 4-3. □: CO_2(g) release after 1 hr photolysis of deareated 0.1 M PA aqueous solutions at 293 K. ○: CO_2(g) release from aqueous 2-acetolactic acid at 293 K.

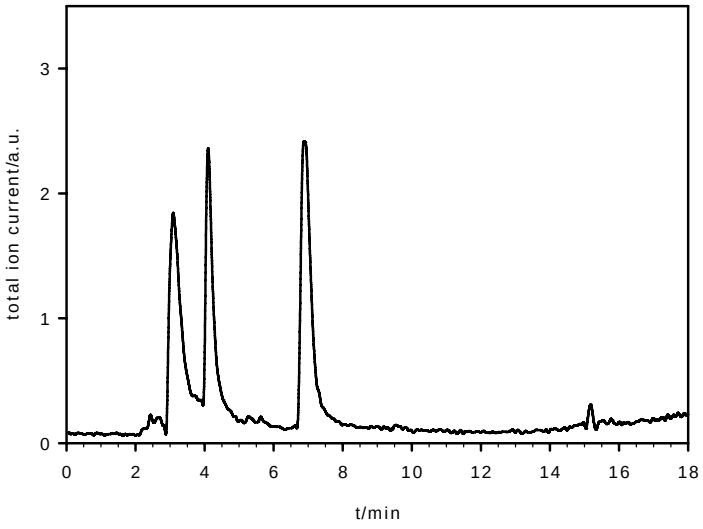

Figure 4-4. Liquid chromatogram of deareated 0.1 M PA solutions after 1 hr photolysis. The species eluting at 3.1, 4.1, and 6.9 min are detected as 87, 177, and 175 Da anions, respectively, via negative ion ESI MS.

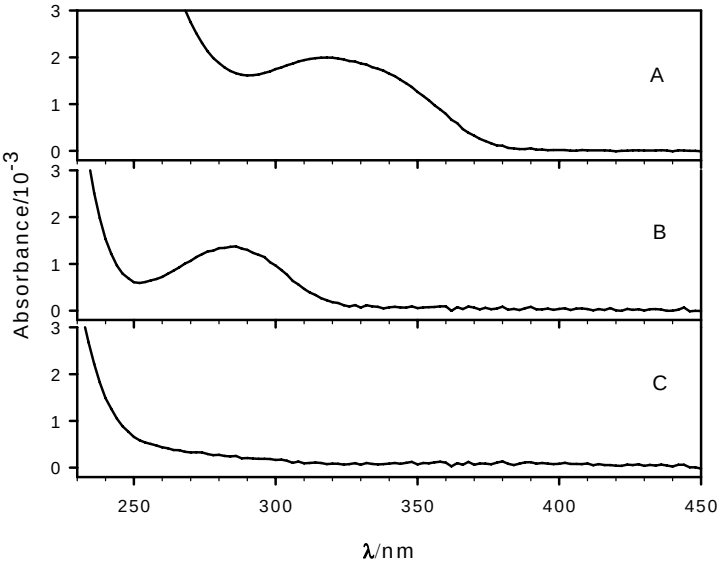

Figure 4-5. UV spectra of the species detected in Fig. 4-4. A: the spectrum of the peaks eluting at 3.1 min. B: at 6.9 min. C: at 4.1 min.

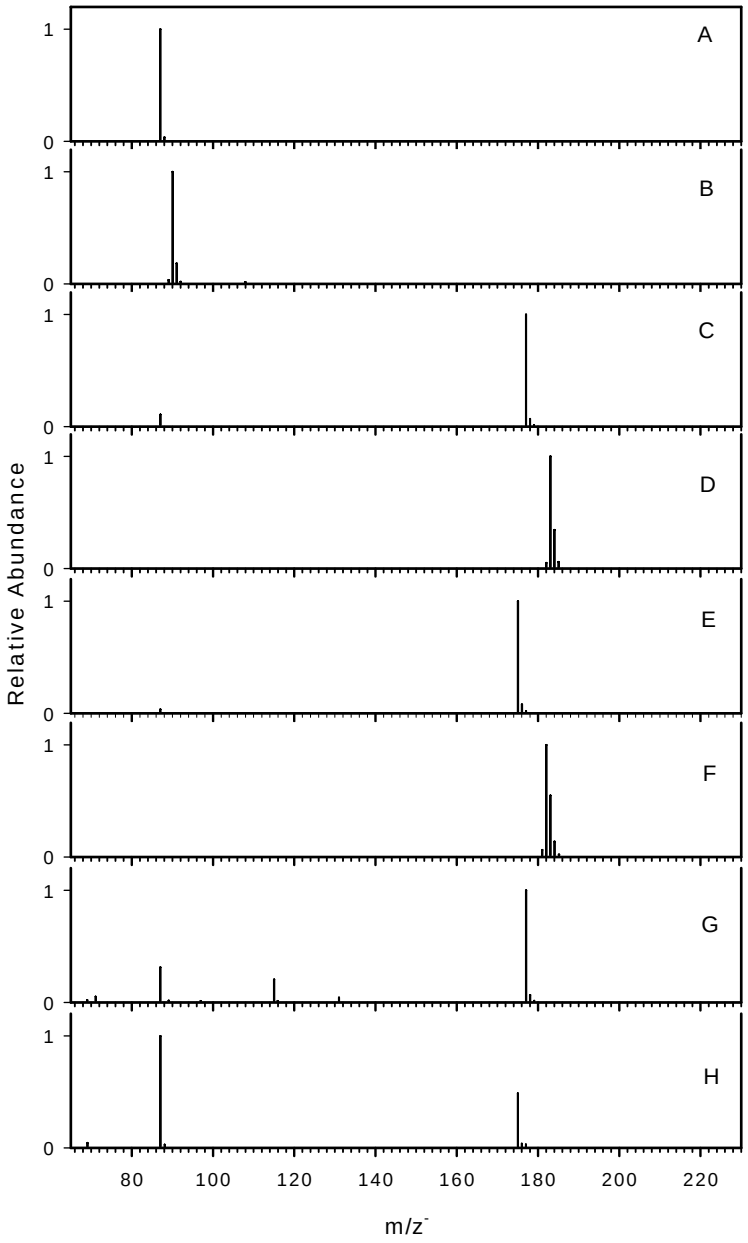

Figure 4-6. ESI MS spectra. A: PA. B: partially deuterated $^{13}C_3$-PA. C: *A* (see Scheme 4-1), the species eluting at 4.1 min in Fig. 4-4. D: same as C but for the photolysis of partially deuterated $^{13}C_3$-PA. E: *B* (see Scheme 4-1), the species eluting at 6.9 min in Fig. 4-4. F: same as E but for the photolysis of partially deuterated $^{13}C_3$-PA. G: the fragmentation spectrum of *A* at 100 V. H: the fragmentation spectrum of *B* at 100 V.

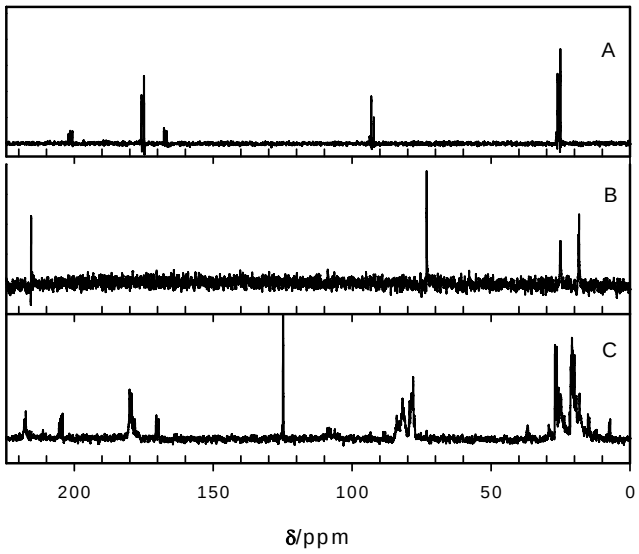

Figure 4-7. ^{13}C NMR spectra. A: $^{13}C_3$-PA. B: 3-hydroxy-2-butanone. C: the photolyzate of deareated 0.1 M $^{13}C_3$-PA after 2 h irradiation.

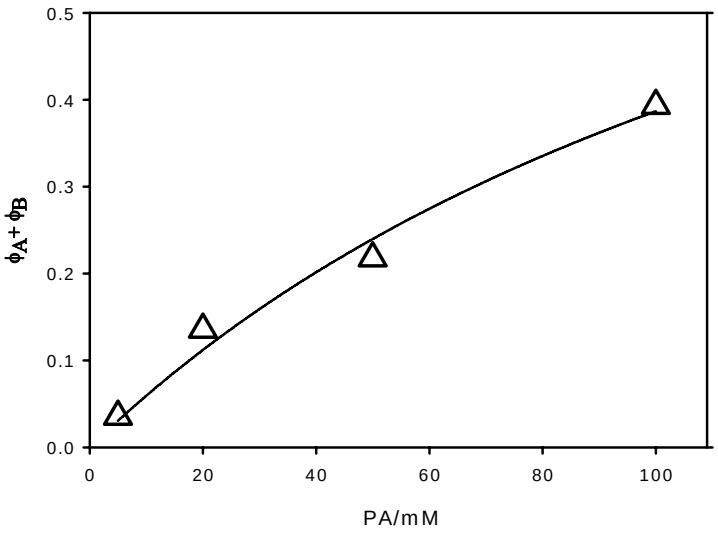

Figure 4-8. Sum of the apparent quantum yields of formation of *A* and *B*, $\phi_A + \phi_B$ vs. [PA] in the photolysis of deareated aqueous PA solutions at 293 K. Quantum yields normalized to the condition $(\phi_A + \phi_B) \rightarrow 1$ as [PA] $\rightarrow \infty$.

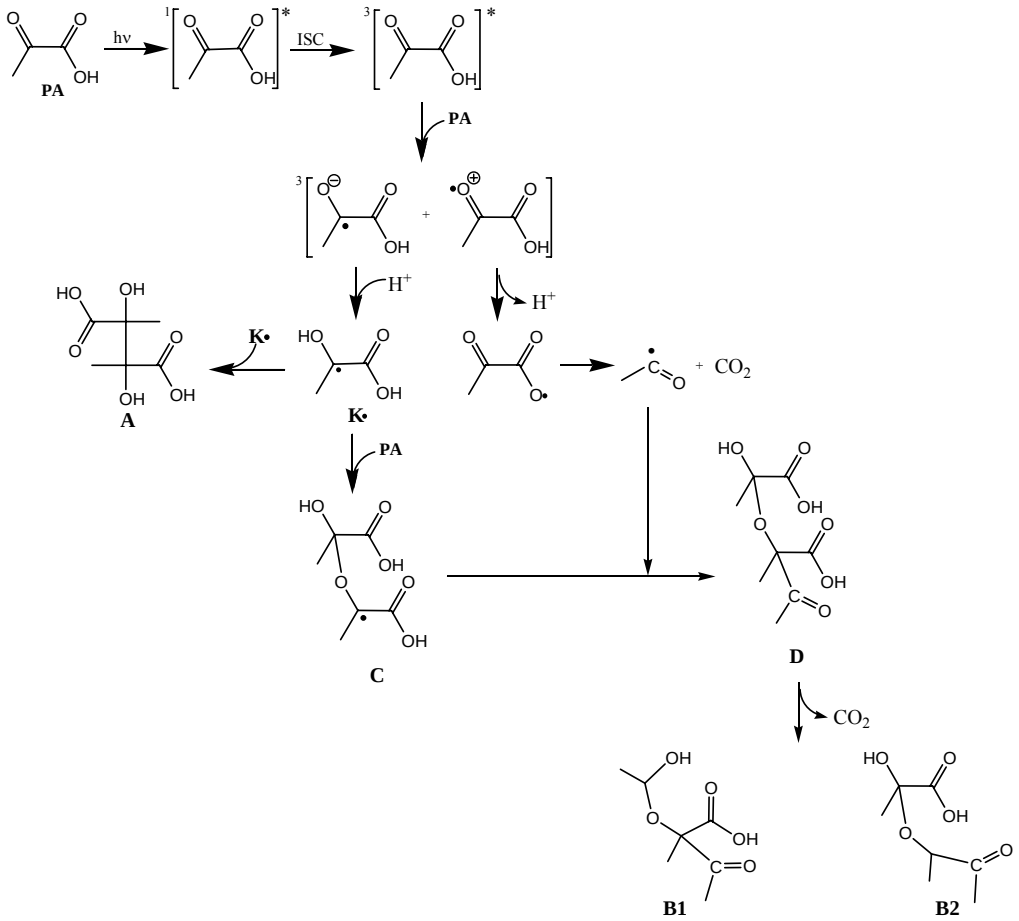

Scheme 4-1

References

1- Moran, M. A.; Zepp, R. G. *Limnol. Oceanogr.* **1997**, *42*, 1307.

2- Andreae, M. O.; Talbot, R. W.; Li, S. M. *J. Geophys. Res.* **1987**, *92*, 6635.

3- Mopper, K.; Zhou, X.; Kieber, R. J.; Sikorski, R. G.; Jones, R. D. *Nature* **1991**, *353*, 60.

4- Kawamura, K.; Imai, Y.; Barrie, L. A. *Atmos. Environ.* **2005**, *39*, 599.

5- Kawamura, K.; Yasui, O. *Atmos. Environ.* **2005**, *39*, 1945.

6- Kawamura, K.; Yokoyama, K.; Fujii, Y.; Watanabe, O. *J. Geophys. Res.* **2001**, *106*, 1131.

7- Kanakidou, M.; Seinfeld, J. H.; Pandis, S. N.; et al., *Atmos. Chem. Phys.* **2005**, *5*, 1053.

8- Miller, W. M.; Zepp, R. G. *Geophys. Res. Lett.* **1995**, *22*, 417.

9- Fisseha, R.; Dommen, J.; Sax, M.; Paulsen, D.; Kalberer, M.; Maurer, R.; Hofler, F.; Weingartner, E.; Baltensperger, U. *Anal. Chem.* **2004**, *76*, 6535.

10- Calvert, J. G. P., J. N. *Photochemistry*; Wiley: New York, 1966.

11- Klotz, B.; Graedler, F.; Sorensen, S.; Barnes, I.; Becker, K. H. *Int. J. Chem. Kinet.* **2001**, *33*, 9.

12- Faust, B. P., K.; Rao, C.; Anastasio, C. *Atmos. Environ.* **1997**, *31*, 497.

13- Buschmann, H. J.; Dutkiewicz, E.; Knoche, W. *Ber. Bunseges. Phys. Chem.* **1982**, *86*, 129.

14- Buschmann, H. J.; Fuldner, H. H.; Knoche, W. *Ber. Bunseges. Phys. Chem.* **1980**, *84*, 41.

15- Leermakers, P. A.; Vesley, G. F. *J. Am. Chem. Soc.* **1963**, *85*, 3776.

16- Budac, D.; Wan, P. *J. Photochem. Photobiolog. A: Chem.* **1992**, *67*, 135.

17- Wan, P.; Budac, D. *CRC Handbook of Organic Photochemistry and Photobiology*; CRC Press: Boca Raton, 1995.

18- Vesley, G. F.; Leermakers, P. A. *J. Phys. Chem.* **1964**, *68*, 2364.

19- O'Neal, J. A.; Kreutz, T. G.; Flynn, G. W. *J. Chem. Phys.* **1987**, *87*, 4598.

20- Turro, N. J.; Weiss, D. S.; Haddon, W. F.; McLafferty, F. W. *J. Am. Chem. Soc.* **1967**, *89*, 3370.

21- Wesdemiotis, C.; McLafferty, F. W. *J. Am. Chem. Soc.* **1987**, *109*, 4760.

22- Gorner, H.; Khun, H. J. *J. Chem. Soc., Perkin Trans., 2* **1999**, 2671.

23- Closs, G. L.; Miller, R. J. *J. Am. Chem. Soc.* **1978**, *100*, 3483.

24- Ronkainen, P.; Brummer, S.; Soumalainen, H. *Acta Chem. Scand.* **1970**, *24*, 3404.

25- Sawaki, Y.; Ogata, Y. *J. Am. Chem. Soc.* **1981**, *103*, 6455.

26- Kendall, D. S.; Leermakers, P. A. *J. Am. Chem. Soc.* **1966**, *88*, 2766.

27- Davidson, R. S.; Goodwin, D. *J. Chem. Soc. Perk. Trans.* **1982**, *2*, 1559.

28- Davidson, R. S.; Goodwin, D.; Fornier de Violet, P. *Chem. Phys. Lett.* **1981**, *78*, 471.

29- Davidson, R. S.; Goodwin, D.; Pratt, J. E. *J. Chem. Soc. Perk. Trans.* **1983**, *2*, 729.

30- Formosinho, S. J. *J. Chem. Soc. Faraday Trans. II* **1976**, *72*, 1313.

31- Eberson, L. *Adv. Phys. Org. Chem.* **1982**, *18*, 79.

32- Cai, Z.; Sevilla, M. D. *Top. Curr. Chem.* **2004**, *237*, 103.

33- Cukier, R. I.; Nocera, D. G. *Annu. Rev. Phys. Chem.* **1998**, *49*, 337.

34- Knoll, H.; Weidemann, F.; Henning, H. *React. Kinet. Catal. Lett.* **1987**, *36*, 411.

35- Kieber, D. J. B., N. V. *Free Rad. Res. Comm.* **1990**, *10*, 109.

36- Kieber, D. J. B., N. V. *Anal. Chem.* **1990**, *62*, 2275.

37- Guzmán, M. I.; Colussi, A. J.; Hoffmann, M. R. *J. Phys. Chem. A* **2006**, *110,* 931.

38- Ronkainen, P.; Brummer, S.; Soumalainen, H. *Anal. Biochem.* **1970**, *34*, 101.

39- NIST. *http://kinetics.nist.gov* **2000**.

40- Defoin, A.; Defoin-Straatmann, R.; Hilderbrand, K.; Bittersmann, E.; Kreft, D.; Khun, H. J. *J. Photochem.* **1986**, *33*, 237.

41- Wagner, P. J.; Zhang, Y.; Puchalski, A. E. *J. Phys. Chem.* **1993**, *97*, 13368.

42- Chiang, Y.; Kresge, A. J.; Pruszynski, P. *J. Amer. Chem. Soc.* **1992**, *114*, 3103.

43- Bandu, M. L.; Watkins, K. R.; Bretthauer, M. L.; Moore, C. A.; Desaire, H. *Anal. Chem.* **2004**, *76*, 1746.

44- Qin, X. Z. *J. Mass Spectrom.* **2003**, *38*, 677.

45- Moe, M. K. *Rapid Commun. Mass Spectrom.* **2005**, *19*, 859.

46- Fischer, G.; Flatau, S.; Schellenberger, A.; Zschunke, A. *J. Org. Chem.* **1988**, *53*, 214.

47- Kimura, H. *J. Polym. Sci., Part A: Polym. Chem.* **1996**, *34*, 3595.

48- Kimura, H. *J. Polym. Sci., Part A: Polym. Chem.* **1998**, *36*, 189.

49- Kimura, H. *Polym. Adv. Technol.* **2001**, *12*, 697.

50- Aylward, G. H.; Findlay, T. J. V. *SI Chemical Data*; Wiley: New York, 1986.

51- Neta, P.; Huie, R. E.; Ross, A. B. *J. Phys. Chem. Ref. Data* **1990**, *19*, 413.

52- Font-Sanchis, E.; Aliaga, C.; Bejan, E. V.; Cornejo, R.; Scaiano, J. C. *J. Org. Chem.* **2003**, *68*, 3199.

53- Scaiano, J. C.; Martin, A.; Yap, G. P. A.; Ingold, K. U. *Org. Lett.* **2000**, *2*, 899.

54- Bejan, E. V.; Font-Sanchis, E.; Scaiano, J. C. *Org. Lett.* **2001**, *3*, 4059.

55- El-Agamey, A.; McGarvey, D. J. *J. Am. Chem. Soc.* **2003**, *125*, 3330.

56- Saxena, P.; Hildemann, L. M. *Environ. Sci. Technol.* **1997**, *31*, 3318.

57- Jang, M.; Czoschke, N. M.; Northcross, A. L. *ChemPhysChem* **2004**, *5*, 1646.

58- Davidson, R. S.; Goodwin, D.; Turnock, G. *Tetrahedron Lett.* **1980**, *21*, 4943.

59- Liu, X. G., M. L.; Wenthold, P. G. *J. Phys. Chem. A* **2005**, *109*, 2183.

60- Griesbeck, A. G.; Kramer, W.; Oelgemoller, M. *Synlett.* **1999**, 1169.

61- Abel, B.; Assmann, J.; Buback, M.; Grimm, C.; Kling, M.; Schmatz, S.; Schroeder, J.; Witte, T. *J. Phys. Chem. A* **2003**, *107*, 9499.

62- Bockman, T. M.; Hubig, S. M.; Kochi, J. K. *J. Org. Chem.* **1997**, *62*, 2210.

63- Step, E. N.; Buchachenko, A. L.; Turro, N. J. *J. Am. Chem. Soc.* **1994**, *116*, 5462.

64- Step, E. N.; Buchachenko, A. L.; Turro, N. J. *J. Org. Chem.* **1992**, *57*, 7018.

65- Nakao, L. S.; Kadiiska, M. B.; Mason, R. P.; Grijalba, M. T.; Augusto, O. *Free Radical Biology & Medicine* **2000**, *29*, 721.

66- Fischer, H.; Paul, H. *Acc. Chem. Res.* **1987**, *20*, 200.

67- Schuchmann, M. N.; von Sonntag, C. *J. Amer. Chem. Soc.* **1988**, *110*, 5698.

68- Negron-Mendoza, A.; Albarran, G. *Radiat. Phys. Chem.* **1990**, *35*, 469.

69- Negron-Mendoza, A.; Castillo, S.; Torres, J. L.; Albarran, G. *Radiat. Phys. Chem.* **1988**, *31*, 825.

70- Martin, C.; Huser, H.; Servat, K.; Kokoh, K. B. *Electrochim. Acta* **2005**, *50*, 2431.

71- Guthrie, J. P. *Bioorg. Chem.* **2002**, *30*, 32.

72- Huang, C. L.; Wu, C. C.; Lien, M. H. *J. Phys. Chem. A* **1997**, *101*, 7867.

73- Sayre, L. M.; Jensen, F. R. *J. Org. Chem.* **1978**, *43*, 4700.

74- Adams, G. E.; Willson, R. L. *J. Chem. Soc. Faraday Trans. 1* **1973**, *69*, 719.

75- von Sonntag, C.; Schuchmann, M. N. *Angew. Chem. Int. Ed. Engl.* **1991**, *30*, 1229.

76- Mezyk, S. P.; Cooper, W. J.; Madden, K. P.; Bartels, D. M. *Environ. Sci. Technol.* **2004**, *38*, 3161.

77- Denisova, T. G.; Denisov, E. T. *Petroleum Chemistry* **2005**, *45*, 26.

78- Samuni, A.; Behar, D.; Fessenden, R. W. *J. Phys. Chem.* **1973**, *77*, 777.

79- Colussi, A. J. *Chemical Kinetics of Small Organic Radicals*; CRC: Boca Raton, Fl., 1988; Vol. 1.

80- Jockusch, S.; Turro, N. J. *J. Am. Chem. Soc.* **1999**, *121*, 3921.

81- Faraji, H.; Lindsay, R. C. *J. Agric. Food Chem.* **2005**, *53*, 736.

82- Yadav, P.; Rao, B. S. M.; Batchelor, S. N.; O'Neill, P. *J. Phys. Chem. A* **2005**, *109*, 2039.

83- Gillbe, C. E.; Sage, F. J.; Gutteridge, J. M. C. *Free Rad. Res.* **1996**, *24*, 1.

84- Morelli, R.; Russo-Volpe, S.; Bruno, N.; Lo Scalzo, R. *J. Agric. Food Chem.* **2003**, *51*, 7418.